



LAWRENCE
LIVERMORE
NATIONAL
LABORATORY

Structure and Origins of Trends in Hydrological Measures over the western United States

T. Das, H. G. Hidalgo, M. D. Dettinger, D. R. Cayan , D.
W. Pierce, C. Bonfils, T. P. Barnett, G. Bala, A. Mirin

September 5, 2008

Journal of Hydrometeorology

Disclaimer

This document was prepared as an account of work sponsored by an agency of the United States government. Neither the United States government nor Lawrence Livermore National Security, LLC, nor any of their employees makes any warranty, expressed or implied, or assumes any legal liability or responsibility for the accuracy, completeness, or usefulness of any information, apparatus, product, or process disclosed, or represents that its use would not infringe privately owned rights. Reference herein to any specific commercial product, process, or service by trade name, trademark, manufacturer, or otherwise does not necessarily constitute or imply its endorsement, recommendation, or favoring by the United States government or Lawrence Livermore National Security, LLC. The views and opinions of authors expressed herein do not necessarily state or reflect those of the United States government or Lawrence Livermore National Security, LLC, and shall not be used for advertising or product endorsement purposes.

1
2
3
4
5
6
7
8
9
10
11
12
13
14
15
16
17
18
19
20
21
22
23
24
25

**Structure and Origins of Trends in Hydrological Measures over the western
United States**

Das T.¹, Hidalgo H.G.¹, Dettinger M.D.^{2,1}, Cayan D.R.^{1,2}, Pierce D.W.¹, Bonfils C.³, Barnett T.
P.¹, Bala G.^{3,4}, Mirin A.³

- 1) Scripps Institution of Oceanography, La Jolla, California, U.S.A.
- 2) United States Geological Survey, La Jolla, California, U.S.A.
- 3) Lawrence Livermore National Laboratory, Livermore, California, U.S.A.
- 4) Centre for Atmospheric and Oceanic Sciences, Indian Institute of Science, India

Submitted to Journal of Hydrometeorology
August 21 2008

1 **Abstract**

2This study examines, at 1/8 degree spatial resolution, the geographic structure of observed trends
3in key hydrologically relevant variables across the western United States (U.S.) over the period
41950-1999, and investigates whether these trends are statistically significantly different from
5trends associated with natural climate variations. A number of variables were analyzed, including
6late winter and spring temperature, winter-total snowy days as a fraction of winter-total wet days,
71st April Snow Water Equivalent (SWE) as a fraction of October through March precipitation
8total (P_{ONDJFM}), and seasonal (January-February-March; JFM) accumulated runoff as a fraction
9of water year accumulated runoff. The observed changes were compared to natural internal
10climate variability simulated by an 850-year control run of the CCSM3-FV climate model,
11statistically downscaled to a 1/8 degree grid using the method of Constructed Analogues. Both
12observed and downscaled temperature and precipitation data were then used to drive the Variable
13Infiltration Capacity (VIC) hydrological model to obtain the hydrological variables analyzed in
14this study. Large trends (magnitudes found less than 5% of the time in the long control run) are
15common in the observations, and occupy substantial part of the area (37 – 42%) over the
16mountainous western U.S. These trends are strongly related to the large scale warming that
17appears over 89% of the domain. The strongest changes in the hydrologic variables, unlikely to
18be associated with natural variability alone, have occurred at medium elevations (750 m to 2500
19m for JFM runoff fractions and 500 m -- 3000 m for $\text{SWE}/P_{\text{ONDJFM}}$) where warming has pushed
20temperatures from slightly below to slightly above freezing. Further analysis using the data on
21selected catchments across the simulation domain indicated that hydroclimatic variables must
22have changed significantly (at 95% confidence level) over at least 45% of the total catchment
23area to achieve a detectable trend in measures accumulated to the catchment scale.

1 **1 Introduction**

2A growing number of studies have investigated recent trends in the observed (and simulated)
3hydro-meteorological variables across the western U.S. The main changes observed in this
4region include a large increase of winter and spring temperatures (Dettinger and Cayan, 1995;
5Károly et al. 2003; Bonfils et al. 2008a; 2008b), a substantial decline in the volume of snow pack
6in low and middle altitudes (Lettenmaier and Gan 1990; Dettinger et al. 2004, Knowles and
7Cayan, 2004; Hamlet et al. 2005), a significant decline in April 1st Snow Water Equivalent
8(SWE; Mote 2003; Mote et al. 2005; Mote 2006; Mote et al. 2008; Pierce et al. 2008), and a
9reduction in March snow cover extent (Groisman et al. 2004). A reduction of the proportion of
10precipitation falling as snow instead of rain has also been observed (Knowles et al. 2006), as well
11as an earlier streamflow from snow dominated basins (Dettinger and Cayan, 1995; Cayan et al.
122001; Stewart et al. 2005; Regonda et al. 2005), and a sizeable increase of winter streamflow
13fraction (Dettinger and Cayan, 1995; Stewart et al. 2005). These changes are likely to have
14important impacts on western U.S. water resources management and distribution if they continue
15into future decades, as is projected for greenhouse-forced warming trends (Barnett, et al. 2004;
16Christensen et al. 2004; 2007; Cayan et al. 2008a; 2008b). This is because much of the water in
17the western U.S. is stored as snow in winter, which starts to melt during late spring and early
18summer. Due to earlier snowmelt and more precipitation falling as liquid instead of stored as
19snow, there could be new stresses on the existing water resources management structures in the
20western U.S. in coming decades.

21

22Some of these studies have indicated that such changes are partially linked with rising
23greenhouse gas concentrations, which alter temperature and thus affect the snow pack
24distribution in the western U.S., and partly from natural climatic decadal fluctuations over the

1North Pacific Ocean (Dettinger and Cayan, 1995). Pacific Decadal Oscillation (PDO; Mantua et
2al. 1997) fluctuations, the dominant decadal natural variability in this region, however can only
3partially explain the magnitude of the recent changes in snowfall fractions (Knowles et al. 2006),
4spring snow pack (Mote et al. 2005) and center timing from snow-dominated basins (Stewart et
5al. 2005). Knowles et al. (2006), Mote et al. (2005) and Stewart et al. (2005) argued that the
6remaining parts of the variability might be due to large-scale anthropogenic warming.

7

8Only recently have formal efforts been undertaken (Knutson et al. 1999; Karoly et al. 2003;
9Maurer et al. 2007 and Bonfils et al. 2008a) to distinguish whether the recent changes occurred
10due to internal natural variations of the climate system or human influence using rigorous
11detection-and-attribution procedures (Hegerl et al. 1996; 1997; Barnett et al. 2001; Zwiers and
12Zhang, 2003; The International Ad Hoc Detection and Attribution Group, 2005; Zhang et al.,
132007; Santer et al. 2007). In formal terms, detection is the determination that a particular climate
14change or sequence is unlikely to have occurred solely due to natural causes. In the present
15study, climate from a long control run of a climate model is used to characterize the kinds of
16long-term variations that can arise solely from the internal fluctuations of the global climate
17system. Other external but natural forcings of the climate system, like solar-irradiance changes
18and volcanic emissions, cannot be tested with available control runs of sufficient length
19(although Barnett et al. (2008) tested hydroclimatic trends from a simulation with climate forced
20only by historical solar and volcanic influences and found that observed trends could not be
21attributed to those influences). Attribution (not undertaken here) is a later step in which the
22particular causes of the “unnatural” parts of observed trends are rigorously identified. Detection
23studies are important because if the recent changes are found to be due to internal natural

1variations alone, one can reasonably anticipate that the climate system will return to its past
2states after some time has passed.

3

4Karoly et al. (2003) carried out a comparison of temperature trends in observations and three
5model simulations at the scale of Northern America. They found that the temperature changes
6from 1950 to 1999 were unlikely to be due to natural climate variation alone, while most of the
7observed warming from 1900 to 1949 was naturally driven. Accounting for uncertainties in the
8observational datasets, Bonfils et al. (2008a) observed noticeable increases in California-
9averaged annual mean temperature for the time periods 1915-2000 and 1950-1999. These
10warmings are too large and too prolonged to have likely been caused by natural variations alone.
11In this study, natural variations were characterized using a long control (no change in
12greenhouse-gas concentrations) simulation by global climate models to develop multi-model 86-
13year and 50-year trend distributions. The authors also indicated that the recent warming in
14California is particularly fast in winter and spring and is likely associated with human-induced
15changes in large-scale atmospheric circulation pattern occurring over the North Pacific Ocean.
16The hypothesis that human activities have influenced the circulation over the North Pacific
17Ocean is strengthened by a recent study (Meehl et al. 2008) that has identified an anthropogenic
18component in the phase shifts of the PDO mode.

19

20More recently, a series of three formal fingerprint-based detection and attribution studies have
21been performed for the western U.S. region. These studies have focused on various late winter
22/early spring hydrologically-relevant temperature variables (Bonfils et al. 2008b), SWE as a
23fraction of precipitation (SWE/P; Pierce et al. 2008) over nine mountainous regions, and center
24timing of stream flow (CT; defined as the day when half of the water year flow has passed a

1given point) in three major tributaries areas of the western U.S. (California region represented by
2the Sacramento and San Joaquin rivers, Colorado at the Lees Ferry and Columbia at The Dalles;
3Hidalgo et al. 2008b). Bonfils et al. 2008b showed that the changes in the observed temperature-
4based indices across the mountainous regions are unlikely, at a high statistical confidence, to
5have occurred due to natural variations. They concluded that changes in the climate due to
6anthropogenic greenhouse gasses (GHGs), ozone, and aerosols are causing part of the recent
7changes. Similarly, Pierce et al. (2008) and Hidalgo et al. (2008b) showed that the observed
8changes in SWE/P and in CT are unlikely to have arisen exclusively from natural internal
9climate variability. Barnett et al. (2008) performed a multiple variable detection and attribution
10study and showed how the changes in minimum temperature (T_{min}), SWE/P and CT for the
11period 1950-1999 co-vary. They concluded, with a high statistical significance, that up to 60% of
12the climatic trends in those variables are human-related.

13

14In regions with complex topography such as the western U.S., there are strong gradients in
15temperature and associated hydrologic structure. These gradients motivate investigating
16responses to climate variability and climate change at high resolution (e.g., ~12 km) scales that
17are much finer than are provided by global climate models. However, the detection of climate
18change at fine scales may be challenging because less averaging means “weather noise”
19increases with decreasing scale (Karoly and Wu, 2005). Consequently, the majority of the
20previous works on detection study have been performed on global, continental or sub-continental
21scale. On the other hand, when a variety of elevational settings are lumped together, the response
22to warming may be diluted because of the strong variations that are mixed together. For example,
23while Hidalgo et al. (2008b) were able to detect fractional runoff changes that were different
24from background natural variability at a high level of confidence in the Columbia basin, changes

1 aggregated over the California Sierra Nevada and in the Colorado basins were only marginally
2 significant or not at all. Maurer et al. (2007) examined whether the decreases in CT at four river
3 points in the Sierra Nevada are statistically significantly different from changes associated with
4 internal natural variability, and concluded that the recent observed trends are still within
5 simulated natural variations. This suggests that, in settings that contain strong topographic
6 variation, it may be useful to evaluate climate responses at finer, rather than coarser spatial units,
7 despite the increase in weather noise.

8

9 The present study investigates the hypothesis that there are detectable climate changes that can
10 be delineated over a complex topographic setting using a high resolution 1/8 degree (~ 12 km
11 resolution) spatial network over the western U.S. (Fig. 1a). Because of the increased signal to
12 noise issues that plague evaluations at this scale, we do not attempt to formally attribute the
13 causes of the unnatural trends at every grid cell. Rather, we use fine resolution simulations to
14 investigate the spatial structure of detectable trends across the snow-dominated western U.S..
15 Our objective is to find the fraction of the regions of the western U.S. where we should expect to
16 see detectably unnatural trends. We focus on some simple indices, which are hydrologically
17 relevant in the area of interest, including late winter and spring temperature, winter-total snowy
18 days as a fraction of winter-total wet days, 1st April Snow Water Equivalent as a fraction of
19 October through March precipitation total, and seasonal runoff fraction. Although global climate
20 changes have been well described in the literature, and even some regional ones, for many
21 applications, such as regional water management, studies of ecosystem diversity, and
22 anticipation of wildfires, finer spatial detail is needed. We also extend the analysis to investigate
23 the fraction of grid cells within a catchment that are required to exhibit detectable changes in
24 order to achieve detectability from the catchment-aggregated runoff and other measures. This

1would provide a useful rule of thumb for many practical purposes, such as designing monitoring
2networks or helping to decide whether detectable trends in a catchment of interest should even be
3expected.

4

5This article is organized as follows. Section 2 presents the data sets and models used in our
6study. A description on the methodology and definitions of various climate indices analyzed in
7this study are given in section 3. Section 4 presents results we have obtained for the different
8indices analyzed. The relationship between total significant area and detectability at catchment
9scale is also presented in Section 4. A summary and conclusions are given in section 5.

10

11 **2 Data Sets and Models**

12 **2.1 Observed data and Global climate model results**

13Gridded meteorological observations were used to characterize observed climate changes across
14the western U.S. over the period 1950-1999. Daily precipitation, maximum and minimum
15temperature observations at 1/8 degree spatial resolution were obtained from the Surface Water
16Modeling Group at the University of Washington (<http://www.hydro.washington.edu>; Hamlet
17and Lettenmaier, 2005). In order to investigate the sensitivity of the results to the meteorological
18observational datasets (used to drive a hydrological model), we repeated the analysis using a
19different version, the Maurer et al. (2002) dataset, which did not include any form of adjustment
20for temporal inhomogeneities. Our conclusions remained insensitive to the choice of the
21observational dataset used. In the following sections, only the results using the Hamlet and
22Lettenmaier (2005) dataset are presented, because this dataset was produced with attention to
23accounting for station and instrument changes that would otherwise add non-climatic noise to the
24long-term trend signal (Hamlet and Lettenmaier, 2005).

1 Internal climate variability in western U.S. in the absence of any anthropogenic effects is
2 characterized using precipitation and temperature data from an 850-year pre-industrial control
3 simulation of the NCAR/DOE Community Climate System Model (CCSM3; Collins et al. 2007).
4 The simulation was performed at Lawrence Livermore National Laboratory and used the Finite
5 Volume (FV) dynamical methods for the atmospheric transport (CCSM3-FV; Bala et al. 2008a;
6 2008b). The horizontal spatial resolution of the atmospheric model was 1×1.25 degree with 26
7 vertical levels. This pre-industrial control simulation used constant 1870-level atmospheric
8 composition to force the model. Bala et al. (2008a) have evaluated the fidelity of a 400-year
9 present day control climate simulation that used this FV configuration for CCSM3. They found
10 significant improvement in the simulation of surface wind stress, sea surface temperature and sea
11 ice when compared to a spectral version of CCSM3.

12

13 **2.2 Downscaling of the control run**

14 Daily precipitation total (P) and daily maximum and minimum temperatures (Tmax, Tmin) from
15 the CCSM3-FV model were downscaled to $1/8$ degree resolution using the Constructed
16 Analogues (CANA; Hidalgo et al. 2008a) statistical downscaling method. The CANA procedure
17 starts with a simple variance correction to ensure the same variability of the GCM data as
18 observations. Then, the bias-corrected global model fields are downscaled using a linear
19 combination of previously observed patterns¹ (Maurer and Hidalgo, 2008; Hidalgo et al. 2008a).
20 The 30 most similar previously observed patterns are used in a linear regression to obtain an
21 estimate that best matches, on the coarse grid, the GCM pattern to be downscaled. The
22 downscaled values of precipitation and temperatures are obtained by applying the linear
23 regression coefficients to the fine scale versions of the previously observed patterns. Results

¹ The coarsened gridded meteorological observations of Maurer et al. (2002) from the period 1950 to 1976 and their corresponding high resolution patterns were used as the library.

1 using CANA and those obtained with another statistical downscaling methodology (bias
2 correction and spatial downscaling; Wood et al. 2004), are qualitatively similar (Maurer and
3 Hidalgo, 2008). An advantage of the CANA method over the bias correction and spatial
4 downscaling method is that CANA can capture changes in the diurnal cycle of temperatures; the
5 downside is that to do this it requires daily data rather than monthly. Details of the CANA
6 method can be found in Hidalgo et al. (2008a).

7

8 **2.3 Hydrological model**

9 Runoff and SWE, major variables of interest to hydrological studies, have not been readily
10 observed at the temporal and spatial scales required for this study. Likewise, they cannot be
11 obtained by downscaling global model results, since no library of observed fine-resolution daily
12 fields exist to use in the downscaling scheme. Accordingly, to produce both the “observed” and
13 climate model driven SWE and runoff fields on the fine spatial scale, we use the Variable
14 Infiltration Capacity (VIC; Liang et al. 1994; 1996) model (version 4.0.5 Beta release 1). To
15 estimate the “observed” trends, we drove VIC with observed daily P, Tmin, and Tmax fields on
16 the 1/8 degree grid; to estimate the downscaled climate model trends, we drive VIC with the
17 downscaled model daily P, Tmin, and Tmax fields on the 1/8 degree grid. VIC uses a tiled
18 representation of the land surface within each model grid cell and allows sub-grid variability in
19 topography, infiltration and land surface vegetation classes (Maurer et al. 2002). The sub-
20 surfaces are modeled using three soil layers with different thickness. Surface runoff uses an
21 infiltration formulation based on the Xinanjiang model (Wood et al. 1992), while baseflow
22 follows the ARNO model (Liang et al. 1994). Sub-grid variability in soil moisture storage
23 capacity is represented through the use of a spatial probability distribution function, and a
24 nonlinear function is used to model the baseflow component from the lowest soil layer (Liang et

1al. 1994; Sheffield et al. 2004). VIC has been successfully applied at spatial scales ranging from
2regional to global (Hamlet et al. 1999; Nijssen et al. 2001; Maurer et al. 2002; Christensen et al.
32004; Wood et al. 2004; Christensen and Lettenmaier, 2007; Hamlet et al. 2007; Maurer 2007;
4Sheffield and Wood, 2007; Barnett et al. 2008; Hidalgo et al. 2008b and Pierce et al. 2008).

5

6The calibrated soil parameters for VIC were obtained from Andrew W. Wood at the University
7of Washington, presently at 3 Tier Group, Seattle (personal communication, 2007). The
8vegetation cover was obtained from the North American Land Data Assimilation System
9(NLDAS). The VIC model was run at a daily time step with the settings of 1-hour snow model
10time step, and five snow elevation bands. The first 9 months of the simulations were used for
11model initializations and were not considered for further analysis, as suggested by Hamlet et al.
12(2007). A number of variables, including runoff, baseflow, soil moisture at three soil layers and
13SWE were produced by the VIC model using the gridded observed and model control run
14meteorologies along with the physiographic characteristics of the catchment (for example soil
15and vegetation). The ability of the model to simulate monthly streamflow at some of the
16calibration points across the study domain is satisfactory when compared with the naturalized
17streamflow (Maurer et al. 2002; Hamlet et al. 2007; and see Fig. 3 Hidalgo, et al. 2008b).
18Additionally, Mote et al. 2005 found reasonable agreement between the spatial pattern of
19observed SWE and the VIC simulated values.

20

21 **2.4 Definition of climate variables**

22Our study focused on 5 hydrologically relevant detection variables:

- 23- Monthly and seasonal precipitation as a fraction of total precipitation over the water year
24 (October through September).

- 1- Monthly and seasonally averaged temperatures.
- 2- Seasonal (January-February-March) accumulated runoff (as simulated by VIC), calculated as
- 3 the fraction of accumulated runoff over the water year.
- 4- 1st April SWE as a fraction of October through March precipitation total (SWE/P_{ONDJFM}),
- 5 chosen to reduce the influence of precipitation on snowpack and produce a snow-based
- 6 climate index that is more directly sensitive to temperature changes (Pierce et al. 2008).
- 7- The number of winter days with precipitation occurring as snow divided by the total number
- 8 of winter days with precipitation. A given wet day (day with precipitation above 0.1 mm), in
- 9 the period November through March, was classified as a snowy day if the amount of snowfall
- 10 (S) was greater than 0.1 mm. S was calculated using the same equation as VIC:

$$S = \begin{cases} 0 & \text{for } T \geq T_{rain} \\ P \cdot \left(\frac{T - T_{rain}}{T_{snow} - T_{rain}} \right) & \text{for } T_{snow} < T < T_{rain} \\ P & \text{for } T \leq T_{snow} \end{cases} \quad (1)$$

11

12 Where, T is the daily average temperature, T_{snow} is the maximum temperature at which snow can
 13 fall and T_{rain} is the minimum temperature at which rain can fall. To be consistent with the VIC
 14 model simulations, the values of T_{snow} and T_{rain} were set to -0.5°C and 0.5°C respectively.

15

16 **2.5 Natural variability in the control run**

17 The strength of the conclusions of any detection analysis rely on the ability of the control model
 18 to represent the strength and key features of the natural internal climate variability in the absence
 19 of anthropogenic effects. In particular, the ability to simulate decadal variability is crucial for the
 20 identification of slow-evolving climate responses to slow-evolving external forcings. To
 21 compare the low-frequency variability in the model control run simulation to observations, we

1 computed standard deviations in each grid cell for each index after application of a 5-year low-
2 pass filter. The observations were linearly detrended before the calculation in an attempt to
3 remove the linear part of possible anthropogenic influence. The low-frequency variability in the
4 control simulation is reasonably well represented with no evidence that the model systematically
5 under- or over-estimate the observed variability for all climate indices (Fig. 2). Thus, we
6 concluded that the CCSM3-FV model used here provide an adequate representation of natural
7 internal climate variability for our detection work. Barnett et al. (2008), Pierce et al. (2008) and
8 Bonfils et al. (2008b) have also addressed this issue using the CCSM3-FV data (i.e., Barnett et
9 al. 2008 Fig. S3) and found similar conclusions.

10

11 **3 Methodology**

12 At each grid cell and for each variable, the linear trend over 50-year segments (with the start of
13 each segment offset by 10 years from the previous segment's start) was calculated from the 850-
14 year control run. This produced 80 partially overlapping estimates of what the 50-year trend
15 could be in the absence of anthropogenic forcing. An Anderson-Darling test² (Anderson and
16 Darling, 1952) showed that the distribution of control run trends was Gaussian in the great
17 majority of the grid cells, except for some grid cells of the JFM runoff fractions. Accordingly,
18 we used the mean and standard deviation from the control run to fit a Gaussian distribution at
19 each grid cell.

20

21 We evaluated the observed trends mainly over the interval of water years 1950-1999 and later
22 over different starting and ending years within this period. The probability of finding the

² The Anderson-Darling test is a modification of Kolmogorov-Smirnov test in which a test statistic (p) was calculated to assess whether the distribution of the trends in the climate indexes computed using the control run data were drawn from a population with a normal distribution. The null hypothesis that the data (trends in the climate indexes computed using the control run) came from a normal distribution was rejected when the calculated p-value was less than a chosen alpha (0.05).

1observed trend in the estimated Gaussian distribution of unforced trends is computed using a
2two-tailed test. We used a two-tailed test because we did not make any *a priori* assumption on
3the direction of the trends of the indices analyzed, since we wanted to evaluate, for example, a
4significant lack of negative temperature trends as well as a significant surplus of positive
5temperature trends. Fig. 3 shows the schematic diagram of the methodology we employed to
6compute the probability. The bars represent the distribution of the 50-year unforced trends in the
7model control run. If an observed trend (arrow) falls within the shaded region (showing the two-
8tailed $p=0.05$ level), which indicates the amplitude of naturally-driven trends that occur only 5%
9of the time, we can conclude that this trend is unlikely to be the result of internal natural
10variations. Probability maps for each variable were obtained by applying this procedure to all
11grid cells across the western U.S.

12

13We also examined the effect of spatial coherence on our results using a Monte Carlo simulation
14as in Livezey and Chen (1982), and Karoly and Wu (2005). Since there is a high spatial
15coherence of the hydro-meteorological variables, this can lead to spurious detection, as described
16in those references. The Monte Carlo approach we use accounts for the effects of this spatial
17coherence.

18

19Because our main focus is to investigate the changes in hydrology, we begin by focusing our
20analysis on the mountainous western U.S., where warming-related impacts are particularly
21important (Mote et al. 2005) and for which hydrological changes may have large implications for
22the water supply, ecology, or likelihood of wildfire in the region. As in Hamlet et al. (2007), we
23include locations where mean April 1st SWE is greater than 50 mm.

24

1In the last section we extend the analysis using the data on the selected catchments across the
2western U.S. to identify relationships, for each of the climate variables, between the fraction of
3catchment area within which significant changes have occurred and the significance of
4detectability at the whole-catchment scale. Such information can be of practical use to resource
5managers trying to understand local climate changes. Trends in 66 catchments across the western
6U.S. were analyzed (Fig. 1a). The areas of the catchments range between 720 km² and 679,248
7km², with a median value of 19,008 km². The average elevations of the catchments range
8between 359 m and 2900 m, with a median value of 1763 m. The catchment-average spring
9(March-April-May) temperatures range between -2 °C and 14 °C, with a median value of 3 °C.

10

11 **4 Results and discussions**

12 **4.1 Spatial pattern of observed trends**

13We analyzed observed monthly precipitation (for January through March) as a fraction of water
14year total precipitation, and monthly average temperatures, for the period 1950 through 1999.
15The trends in monthly precipitation fraction we found were well within the distribution of natural
16variability as estimated from the control model run (not shown). This agrees with the results of
17Barnett et al. (2008), who also found that natural variability could account for changes in water
18year total precipitation for the mountainous western U.S. during this period.

19

20Observations show warming temperatures since 1950 over the western U.S. during the months of
21January, February, and March (Fig. 4a). Among these months, March average temperature shows
22the strongest and most widespread upward trends, with larger warming in the interior west than
23along the coast. Notable warming in January is concentrated along the coast of California region

1and Columbia River basin, and February average temperature shows widespread but only mild
2warming trends; see Knowles et al., 2006, for more detail on these cool-season warming patterns.

3

4In view of the considerable warming trends for the study domain during January and March, we
5investigated changes in observed JFM (January-February-March) average temperature. A linear
6trend calculation using the JFM average temperature shows a considerable upward trend across
7most parts of the snow-dominated western U.S., with notably larger warming trends across the
8high mountains of the Columbia River basin (Fig. 5a).

9

10A chain of hydrologic responses to warming was evident in the trends. Reductions in observed
11winter-total snowy days as a fraction of winter-total days with precipitation (indicating a
12decrease in days with snowfall) are also common across many parts of the snow dominated
13region in the observed simulation, except in regions at the Northern Rockies which show no
14trend (Fig. 5b). There are widespread downward trends in observed SWE/P_{ONDJFM} across most
15parts of the snow dominated western U.S., with stronger downward trends in the northern
16Rockies of the Columbia River basin along with some upward trends at the southern Sierra and
17part of Northern Rockies (Fig. 5c). These findings are in agreement with those of Pierce et al.
18(2008), who described declining fractional SWE/P from snow course data across the nine
19mountainous regions of the western U.S. These trend patterns are also consistent with the results
20in Mote et al. (2005), who analyzed April 1st SWE from 824 snow stations for the period 1950-
211997, and Hamlet et al. (2005), who analyzed VIC simulated April 1st SWE. Using regression
22analyses, those two studies attributed the widespread downward trend in SWE to a warming
23trend, and a more regional upward trend in SWE in the southern Sierra (in the California region)
24to an increase of precipitation over the period. Changes in snowmelt initiation and changes in

1 snow-to-rain ratio should concur with large changes in runoff. Indeed, upward trends in JFM
2 runoff fractions predominate across the snow dominated western U.S., except some weaker
3 downward trends in the Canadian part of the Columbia River basin and Colorado Rockies (Fig.
4 5d).

5

6 **4.2 Comparison of observed trends with model control run trends distribution at the** 7 **grid scale**

8 Figs. 4b and 6 illustrate the probability of the observed trends in Figs. 4a and 5 arising in absence
9 of any external forcings. There are considerable regions over which the observed trends in
10 January and March average temperature are unlikely to have arisen from internal natural
11 variability alone (at 95% significance level) (Fig. 4b). By contrast, the mild warming trends in
12 February are not detectably different from internal natural variability (Fig. 4b)

13

14 The observed trends toward warmer JFM average temperature across nearly all (89%) of the
15 snow-dominated regions of the western U.S. can not be explained (at 95% confidence level) by
16 internal natural variability alone, except relatively small areas of the Southern Sierra (California
17 region) and Southern Rockies (lower Colorado River basin) (Fig. 6a). The downward trends of
18 the snow day fraction of wet days (Fig. 6b) also exhibit detectable signals for many grid cells,
19 42%, over mountainous western U.S.. The decline in SWE/P_{ONDJFM} found in the observations,
20 40% of the snow-dominated grid points, is also unlikely to be associated with natural variations
21 alone in many regions (Fig. 6c). However, opposite changes in regions containing upward trends
22 in SWE/P_{ONDJFM} (e.g., Southern Sierra and Utah) cannot be confidently distinguished from
23 internal natural variability. Consistent with the warming and reduction in fraction of snowy days
24 and SWE/P_{ONDJFM} increases in JFM runoff fraction exceed those expected from natural

1variations alone over substantial mountainous regions, 37% of the snow-dominated grid points,
2especially in the Columbia River basin, (Fig. 6d). Changes in regions such as the Southern Sierra
3(California region) and Southern Rockies (Colorado River basin) cannot be distinguished
4confidently from natural variability.

5

6There is high spatial coherence in the meteorological and hydrological variables, which may
7overstate how widespread the statistically significant trends are (Livezy and Chen, 1982) in Fig.
86. In order to estimate the sampling distribution of the percentage of the grid cells that could
9simultaneously show a statistically significant trend in the model control run, taking the observed
10spatial coherence into account, we have performed a Monte Carlo experiment based on
11resampling from the model control run. We sequentially selected all 800 possible 50-year
12segments (i.e., moving 50-year windows with 1 year shifts) of the 850-year control run and
13computed the probability map from each selection, as done previously with the observations.
14This resulted in 800 probability maps. The fraction of grid cells exhibiting a apparently
15detectable signal (at 95% confidence level) was computed from each probability map, giving us
16800 values with which to estimate the distribution of the fractions of grid cells that might, by
17chance, yield a seemingly detectable signal in a 50-year segment from the control run. Although
18this number would be 5% *on average* over the 850-year control run if all grid cells varied
19independently of each other, the lack of independence between nearby grid cells means that, in
20any particular 50-year segment, either very few or very many grid cells might show seemingly
21significant trends. Consequently, the 95th percentile of this rather wide sampling distribution is
22considerably greater than 5% of the grid cells; the Monte Carlo-derived value is noted for each
23hydroclimatic variable in parenthesis in the panel titles of Fig. 6. The 95th percentile limits are
24still much less than the observed fractions of grid cells exhibiting significant trends for each

1variable, indicating that more grid cells contain significant trends than would be expected by
2chance, even taking the spatial coherence into account (Fig. 6).

3

4An important property of the changes depicted in Fig. 6 is that they depend on elevation. In order
5to illustrate the dependence of the changes on elevation, we computed the total number of
6observed grid cells showing significant trends for each elevation class. Results are shown in Fig.
77, where the grey regions indicate results not significantly different from the control run at the
895% level, based the Monte Carlo resampling. The grey regions include zero; the wideness of the
9sampling distribution, noted above, means that even finding *no* grid cells with a significant trend
10does not indicate a statistically significant *lack* of trends. For example, finding no grid points at
11all with a statistically significant *decrease* in temperature is still consistent with the control run.
12Consequently, all significant results presented here arise from a surfeit of trends, not a deficit of
13trends.

14

15In Fig. 7, red points on the left hand panels show the numbers of positive trends, and blue points
16on the right hand panels show the number of negative trends. The JFM warming (Fig. 7b, left) is
17detectable at all elevations, but the very small number of downward trends is not inconsistent
18with natural variability (Fig. 7b, right). The fraction of cells exhibiting significant upward trends
19decreases monotonically with elevation.

20

21The decline of the snowy days as a fraction of wet days from elevations near sea level up to 3000
22m also exhibits a high tendency of being statistically significantly different from the distribution
23of trends from natural variations alone (Fig. 7c, right panel). Conversely the grid cells with
24increasing trends—which show up mostly in small patches in the Rocky Mountains (e.g., also,

1 Knowles et al 2006) — are not inconsistent with natural variability (Fig. 7c, left panel). The
2 reduction in SWE/P_{ONDJFM} is particularly detectable at the lower elevations, but it is also
3 detectable at medium altitudes (below 3000 m) (Fig. 7d, right panel). The grid cells with positive
4 trends (Fig. 7d left panel) for all elevation classes, and the highest grid cells with negative trends
5 (more than 3000 m), exhibit trends in numbers that could be expected due to natural variability.

6

7 The upward trends in the JFM runoff fractions in the regions with elevation ranging between
8 approximately 750 m to 2500 m tend to be statistically significantly more common than the
9 model estimated natural trends (Fig. 7e, right panel); however, the downward trends for all
10 elevation classes and the upward trends at lower altitudes (lower than 750 m), and higher
11 altitudes (higher than 2750 m) are not statistically significant in numbers than those that would
12 occur due to natural variability (Fig. 7e). Thus JFM runoff fraction trends in the middle
13 elevations—high enough to have significant snowmelt contributions but low enough so that
14 temperatures are close to freezing during critical times—have changed in ways that cannot
15 readily be attributed to natural variability nor to spatial coherence of random occurrences. As
16 noted above, decreasing trends in temperature and runoff, as well as increasing trends in snowy
17 days and SWE/P_{ONDJFM} occur rarely, cannot be shown to be different from natural variability
18 with this data set. However, we did not find precipitation trends to be different from natural,
19 except around elevation 1500 m (Fig. 7a). Thus hydrological trends driven by temperatures are
20 the ones most likely to be unnatural. Previous detection and attribution studies of regionally
21 averaged variables (Barnett et al. 2008; Bonfils et al. 2008b; Pierce et al. 2008; and Hidalgo et al.
22 2008b) have successfully attributed the temperature trends that we detect here at fine scales to
23 forcing from greenhouse gases.

24

Fig. 8 demonstrates another aspect of the hydrological changes – the number of grid cells that show significant trends, stratified by 1950-1999 climatological spring average temperature classes (instead of elevation classes). Trends that tested as having significant magnitudes were nearly all found in locations having mean temperatures above -4°C . Interestingly, the changes for snowy days, $\text{SWE}/\text{P}_{\text{ONDJFM}}$ and runoff fractions are consistent with natural variability for cells where spring temperatures are below -4°C . The results support the findings of Knowles et al. (2006) that showed that regions at low to medium elevations with temperature near freezing are more likely to have a decrease in the fraction of precipitation falling as snow, and also consistent with Mote et al 2005 who found these elevations to have incurred unusual reductions in spring snowpack. Figures 7 & 8 also show that changes in the sense *a priori* expected from warming conditions (for example, a decrease of days with snowfall) are more prevalent than those in the opposite sense. Again, the changes in the JFM precipitation fraction at different temperature ranges are not outside what could be expected due to internal natural variability, except at temperature class -4°C .

15

We also investigated the sensitivity of these results to the time period analyzed. As an example the results from the JFM average temperature are shown in Fig. 9 (a). In this experiment we used three different analysis periods, all starting in 1950, to compute the observed trends: 30 years (1950-1979), 40 years (1950-1989) and 50 years (1950-1999). The results show that the longer periods contain more grid cells exhibiting a detectable warming trend (Fig. 9a, left panel). This is different from what is expected for natural variability in an equilibrated climate system, where the period of averaging will make no systematic difference to the fraction of grid cells deemed to have significant trends. Interestingly, the grid cells located at higher elevations (above approximately 1500 m) exhibit more detectable trends as the time period increases in length.

1Also, the changes at the grid cells located at high elevations are not inconsistent with natural
2variability for the shorter time period (1959-1979) (Fig. 9a, left panel). Two potential reasons
3can explain these results: (a) increases in noise when trends are calculated over shorter time
4periods, or (b) the strength of the trend becomes stronger at the end of the time period (as can
5occur if the climate respond to the slow-evolving anthropogenic forcing).

6

7To investigate these possibilities, we reanalyzed the trends using a fixed period length of 30
8years, but with three different starting years: 1950, 1960 and 1970 (Fig. 9, right panel). Starting
9in 1950, cells with warming that is greater than would be expected locally from the natural
10variability are all below 750 m elevation. In contrast, starting in 1960, grid cells with locally
11detectable warming are above 2250 m, but the Monte Carlo resampling suggests that the
12numbers of trends seemingly distinguishable from natural variability are not, yet, any larger than
13might be expected from the spatially coherent natural-variability fields. Starting in 1970, though,
14cells above 2250 m experienced a detectable warming (Fig. 9a, right panel). Thus the warming
15trends appear to have begun at lower elevations earlier than at higher elevations. Longer
16observational records also contributed to our growing ability to detect the long-term trends.
17Similar patterns were also found in the hydrological variables analyzed in this paper
18(SWE/ P_{ONDJFM} and JFM runoff fractions) (Fig. 9b & Fig. 9c), indicating the crucial role of the
19very longest time series in analyses such as this.

20

21 **4.3 Detection at catchment scale**

22Very often, observations and decisions involving these hydroclimatic trends are addressed to the
23basin scales, rather than to the individual 12-km grid cells analyzed here. For example, runoff is
24measured and managed primarily as streamflow accumulated to the river basin scale rather than

1as a distributed runoff patterns. Thus, in light of the strong elevation dependence of the
2detectability of trends discussed above, it is natural to ask: “How much of a basin must lie within
3these critical elevation bands before the observations from the basin as a whole are likely to
4show detectable trends?” To address this issue and perhaps to develop some rules of thumb for
5where to expect detectability of unnatural trends thus far, we analyze the relations between
6fractions of catchment areas with detectable trends and corresponding detectability of trends at
7the whole-catchment scale.

8

9Trends in 66 catchments across the simulation domain of the western U.S. were analyzed (Fig.
101a). Hydroclimatic variables from all grid cells within a given catchment were averaged for the
11observed (or simulated using the observed meteorology) and control run data. The probabilities
12of any resulting trends of the catchment-averaged observed time series were then computed
13using the same procedure previously applied at the grid-cell scale (described in section 3). The
14detectability of unnatural trends within each catchment-averaged series was then compared to the
15fractions of grid cells within that catchment that were locally detectably distinguishable from the
16control-run natural variability.

17

18This analysis indicates that approximately 25% of the catchment area must have trended
19significantly (at 95% confidence level) before there are detectable changes (at 95% confidence
20level) in the catchment level for snowy days as fraction of wet days and SWE/ P_{ONDJFM} .
21Approximately 45% of the catchment area must have trended significantly before there are
22detectable trends in JFM runoff fractions at the catchment scale (Fig. 10).

23

1 Since we have found that certain elevation zones or average spring temperature bands are most
2 likely to yield detectable trends (thus far), it would be useful to know whether the (known)
3 fraction of a catchment area within these ranges dictates detectability at the catchment scale
4 better than the area with locally “detectable” trends, which generally is not known *a priori*.
5 Unfortunately, no clearly preferred mean spring temperature ranges or elevation ranges that
6 characterize the significant catchment were found, except with respect to JFM runoff fractions.
7 Catchments with significant trends in JFM runoff fractions all have catchment-average spring
8 temperatures between -2°C and 6°C, and those catchments are located at the medium elevation
9 range (approximately ranging between 1400 m and 2500 m). Fractions of catchment areas within
10 such ranges, rather than catchment-average values, did not relate usefully to whole-catchment
11 detectability.

12

13 5 **Summary and conclusions**

14 This study has used a fine-scale ($1/8$ degree \times $1/8$ degree latitude-longitude) analysis of
15 meteorological and hydrological variables to investigate the structure of observed trends from
16 1950-1999 in some key hydrologically relevant measures across the western U.S. Combined with
17 estimates of natural variability from an 850 year GCM control simulation, observations were
18 evaluated to determine which elevations and locations have experienced trends that are unlikely
19 to be derived entirely from internal natural climatic variations. The VIC hydrologic model was
20 used to simulate the surface hydrological variables, both during the observational period (when
21 driven by observed meteorology) and from the global climate models (when driven by
22 downscaled model fields). Using key hydrologic measures, including JFM temperature, fraction
23 of days with snow, SWE/P_{ONDJFM} and JFM runoff fractions, we find that that the observed winter
24 temperature and each of the hydrologic measures have undergone significant trends over

1considerable parts (37 – 89%) of the snow dominated western U.S. (Fig. 6). These trends are not
2likely to have resulted from natural variability alone, as gaged from the distribution of trends
3produced from the long control simulation. In a relatively large portion of the Columbia and to a
4lesser extend in the California Sierra Nevada and in the Colorado River basin, trends in snow
5accumulation and runoff timing across many middle altitudes are unlikely to have been caused
6by natural variations alone (Fig. 7). These trends are caused by warming of regions with mean
7spring temperature close to freezing.

8

9In all cases, the significant changes occurred in a direction consistent with the sign of the
10changes associated with warming. For example, JFM average temperature increases, days with
11snowfall decreases, snowpack decreases, and JFM runoff increases. Reinforcing this result is that
12trends that occurred in the opposite direction are no more frequent than would be expected from
13natural variability, small and non-significant.

14

15For SWE and JFM runoff fractions that we have evaluated here, good observational datasets do
16not exist for the spatial scales we considered. We have used the VIC hydrological model forced
17by observed meteorological conditions to simulate these variables, a limitation of this study that
18should be kept in mind. Though the VIC model performance has been evaluated for the domain
19of interest for a number of variables (Maurer et al. 2002; Mote et al. 2005), there could be
20uncertainties arising from several factors, including lack of ability to simulate accurate observed
21trend, or uncertainties in the preparation of the gridded forcing data set (particularly at the
22mountains due to fewer stations available for the interpolation). There may be some biases due to
23specific stations used to construct the gridded data set. There are many localized ‘point’ trends
24that probably originate at individual stations.

1Experiments that considered different start and end points of the 1950-1999 interval suggest that
2significant warming and associated hydrological trends, not explained by natural variations, have
3begun earlier at lower elevations than at higher elevations. Longer observational records
4contribute a growing ability to detect the trends.

5

6We also analyzed the fine-scale data in snow-influenced catchments across the western U.S. To
7find a detectable trend (at 95% confidence level) at the catchment scale, at least 25% of the total
8catchment area must have trended significantly for snowy days as a fraction of wet days and
9SWE/ P_{ONDJFM} , but at least 45% area for JFM runoff fractions (Fig. 10). These thresholds provide
10a context to understand the behavior observed in the major tributaries areas of the western U.S.
11(used in Barnett et al. 2008 and Hidalgo et al. 2008) (California Sierra Nevada, Colorado at the
12Lees Ferry and Columbia at The Dalles) (as shown in Fig. 1b) as well as many smaller river
13basins. Among the three major tributaries areas analyzed there, the Columbia contains the largest
14percentage area with significant trends for April 1 SWE/ P_{ONDJFM} (decreasing) and for the fraction
15of annual runoff in JFM (increasing), as shown in Table 1. While the portion of the Sierra and
16Colorado with significant trends in these measures is 15%, or less, those in the Columbia exceed
1725%. Stronger signatures observed in the Columbia basin are quite clearly a reflection of the
18greater proportion of low-middle elevations and, in association, a preponderance of late winter
19and early spring temperatures in the sensitive -2°C to $+4^{\circ}\text{C}$ category. Lower to middle altitudes
20(near sea level to nearly 3000 m) of California showed the second highest percentage area
21exhibiting significant trends, but these signals are diluted by the much larger number of grid cells
22that are located in an elevational environment where warming has not been great enough to
23produce a significant effect. Warming of even a few degrees in the higher altitudes, above 3000
24m, where the temperature is currently much below the freezing point in winter is not sufficient

1yet to make detectable changes.

2

3In addition to conducting climate detection on a very fine scale, the present study differs from
4most previous trend significance studies, in which a more traditional significance test (parametric
5or nonparametric) is performed to assess whether or not an observed trend is significantly
6different from zero. Naturally occurring climate phenomena such as the Pacific Decadal
7Oscillation can give statistically significant trends over long periods, so the presence of non-zero
8trends is not necessarily inconsistent with the hypothesis that the trends are caused by natural
9variability. Instead we used long model control simulations to quantify the trends in our variables
10likely to arise from natural internal climate variability, and compared the observed trends to
11those.

12

13The present study yields results, on a fine scale grid, that indicate a positive detection of changes
14in hydrologic variables that could not be expected from natural variability in many sub-areas
15within the western U.S., but we did not conduct experiments to attribute these changes to
16particular external forcings. However, given the conclusions of Barnett et al. (2008), Bonfils et
17al. (2008b), Pierce et al. (2008) and Hidalgo et al. (2008b) using the same domain but at a much
18larger spatial scale (9 regions over the western U.S.), we can reasonably predict that the origin of
19a substantial portion of the trends is anthropogenic warming. If this warming continues into
20future decades as projected by climate models, there will be serious implications for the
21hydrological cycle and water supplies of the western U.S. The present results usefully bring the
22results of regional-scale detection-and-attribution down to scales needed for water management,
23studies of ecosystem diversity, and anticipation of wildfires.

24

25

1 Acknowledgments

2 This work was supported by the Lawrence Livermore National Laboratory through a LDRD
3 grant to the Scripps Institution of Oceanography (SIO) via the San Diego Supercomputer Center
4 for the LUCiD project. The USGS and SIO provided partial salary support for DC and MD; and
5 the California Energy Commission PIER Program, through the California Climate Change
6 Center, provided partial salary support for DC, DP and HH and the NOAA RISA Program
7 provided partial salary support for DC, Mary Tyree and Jennifer Johns at SIO. The Program of
8 Climate Model Diagnosis and Intercomparison (PCMDI) supported CB and GB (the former via a
9 DOE Distinguished Scientist Fellowship awarded to B. Santer). The VIC model calibrated soil
10 parameters were generously provided by Andrew W. Wood at the 3 Tier Group, Seattle, WA
11 198121. The authors thank Mary Tyree for her support in processing some of the data. We thank
12 Jennifer Johns for her comments on the initial version of the manuscript.
13 This work performed under the auspices of the U.S. Department of Energy by Lawrence Livermore
14 National Laboratory under Contract DE-AC52-07NA27344.

15

16

17

18

19

20

21

22

23

24

25

26

27

28

1References

- 2Anderson, T. W. and Darling, D. A., 1952: Asymptotic theory of certain 'goodness-of-fit' criteria
3based on stochastic processes. *Annals of Mathematical Statistics*, 23:193-212.
4
- 5Barnett, T. P., D. W. Pierce, and R. Schnur, 2001: Detection of anthropogenic climate change in
6the world's oceans. *Science*, 292, 270–274.
7
- 8Barnett, T.P., Malone, R., Pennell, W., Stammer, D., Semtner, B., and Washington, W., 2004:
9The effects of climate change on water resources in the west: Introduction and Overview.
10Climatic Change, 62: 1-11.
11
- 12Barnett, T.P., D.W. Pierce, H.G. Hidalgo, C. Bonfils, B. D. Santer, T. Das, G. Bala, A. Wood, T.
13Nazawa, A. Mirin, D. Cayan and M. Dettinger, 2008: Human-induced changes in the hydrology
14of the western US. *Science*, doi:10.1126/science.1152538.
15
- 16Bala, G., R.B. Rood, A. Mirin, J. McClean, K. Achutarao, D. Bader, P. Gleckler, R. Neale and P.
17Rash, 2008a: Evaluation of a CCSM3 simulation with a finite volume dynamical core for the
18atmosphere at 1 deg latitude x 1.25 deg longitude resolution. *J. Climate*, 21, 1467-1486.
19
- 20Bala, G., Rood, R.B., Bader, D., Mirin, A., Ivanova, D., and Drui, C. 2008b: Simulated climate
21near steep topography: Sensitivity to numerical methods for atmospheric transport. *Geophysical*
22*Research Let.* 35, L14807, doi:10.1029/2008GL033204.
23
- 24Bonfils, C., P. Duffy, B. Santer, T. Wigley, D.B. Lobell, T.J. Phillips, and C. Doutriaux, 2008a:
25Identification of external influences on temperatures in California, *Clim. Ch.*, 87(s1), 43-55.
26
- 27Bonfils C., B.D. Santer, D.W. Pierce, H.G. Hidalgo, G. Bala, T. Das, T.P. Barnett, D.R. Cayan,
28C. Doutriaux, A.W. Wood, A. Mirin, T. Nozawa, 2008b: Detection and Attribution of
29temperature changes in the mountainous western United States. *J. Climate*, in press.
30
- 31Christensen, N.S., A.W. Wood, N. Voisin, D.P. Lettenmaier, and R.N. Palmer, 2004: The effects
32of climate change on the hydrology and water resources of the Colorado River basin. *Climatic*
33*Change*, 62(1-3), 337-363.
34
- 35Christensen, N. S. and D.P. Lettenmaier, 2007: A multimodel ensemble approach to assessment
36of climate change impacts on the hydrology and water resources of the Colorado River Basin.
37*Hydrol. Earth Syst. Sci.*, 11, 1417-1434.
38
- 39Cayan, D. R., S. A. Kammerdiener, M. D. Dettinger, J. M. Caprio, and D. H. Peterson, 2001:
40Changes in the onset of spring in the western United States. *Bull. Amer. Meteor. Soc.*, 82, 399–
41415.
42
- 43Cayan, D.R., E.P. Maurer, M.D. Dettinger, M. Tyree and K. Hayhoe, 2008a: Climate change
44scenarios for the California region. *Climatic Change*, Vol. 87, Suppl. 1, 21-42 doi:
4510.1007/s10584-007-9377-6
46

1Cayan, D.R., A.L. Luers, G. Franco, M. Hanemann, B. Croes and E. Vine, 2008b: Overview of
2the California climate change scenarios project. *Climatic Change*, 87, (Suppl 1):S1-S6,
3doi:10.1007/s10584-007-9352-2.

4

5Collins, W. D., C. M. Bitz, M. L. Blackmon, G. B. Bonan, C. S. Bretherton, J. A. Carton, P.
6Chang, S. C. Doney, J. J. Hack, T. B. Henderson, J. T. Kiehl, W. G. Large, D. S. McKenna, B.
7D. Santer, and R. D. Smith. 2007. The Community Climate System Model: CCSM3. *Journal of*
8*Climate CCSM3 special issue*. In press.

9

10Daly, C., Neilson, R.P., and Phillips, D.L. 1994: A statistical-topographic model for mapping
11climatological precipitation over mountainous terrain. *Journal of Applied Meteorology* **33**: 140-
12158.

13

14Dettinger, M. D., and D. R. Cayan, 1995: Large-scale atmospheric forcing of recent trends
15toward early snowmelt runoff in California. *J. Climate*, 8, 606–623.

16

17Dettinger, M. D., D. R. Cayan, M. K. Meyer, and A. E. Jeton, 2004: Simulated hydrologic
18responses to climate variations and change in the Merced, Carson, and American River basins,
19Sierra Nevada, California, 1900–2099. *Climatic Change*, 62, 283–317.

20

21Groisman, P. Y., R. W. Knight, T. R. Karl, D. R. Easterling, B. Sun, and J. H. Lawrimore, 2004:
22Contemporary changes of the hydrological cycle over the contiguous United States: Trends
23derived from in situ observations. *J. Hydromet.*, 5, 64-85.

24

25Hamlet, A. F., and D.P. Lettenmaier, 1999: Effects of climate change on hydrology and water
26resources in the Columbia River basin. *Journal of the American Water Resources Association*,
2735, 1597-1623.

28

29Hamlet A.F. and Lettenmaier D.P., 2005: Production of temporally consistent gridded
30precipitation and temperature fields for the continental U.S. *J. Hydrometeorology* 6 (3), 330-
31336.

32

33Hamlet A.F., P.W Mote, M.P. Clark, and D.P. Lettenmaier, 2007: 20th Century Trends in
34Runoff, Evapotranspiration, and Soil Moisture in the Western U.S. *Journal of Climate* 20(8):
351468-1486.

36

37Hegerl, G. C., H. von Storch, K. Hasselmann, B. D. Santer, U. Cubasch, and P. D. Jones, 1996:
38Detecting greenhouse-gas-induced climate change with an optimal fingerprint method. *J.*
39*Climate*, 9, 2281–2306.

40

41Hegerl, G. C., K. Hasselmann, U. Cubasch, J. F. B. Mitchell, E. Roeckner, R. Voss, and J.
42Waszkewitz, 1997: Multi-fingerprint detection and attribution of greenhouse-gas and aerosol-
43forced climate change. *Climate Dyn.*, 13, 613–634.

44

45Hidalgo, H. G., M. D. Dettinger, and D. R. Cayan, 2008a: Downscaling with constructed
46analogues: Daily precipitation and temperature fields over the United States. California Energy
47Commission, PIER Energy-Related Environmental Research. CEC-500-2007-123. Available on-

1line: <http://www.energy.ca.gov/2007publications/CEC-500-2007-123/CEC-500-2007-123.PDF>.
248 pp.
3
4Hidalgo, H.G., T. Das, M.D. Dettinger, D.R. Cayan, D.W. Pierce, T.P. Barnett, G. Bala, A.
5Mirin., A.W. Wood, C.Bonfils, B.D. Santer, T. Nozawa, 2008b: Detection and Attribution of
6Climate Change in Streamflow Timing of the Western United States. J. Climate, in review.
7
8Karoly, D. J., and Q. Wu., 2005: Detection of regional surface temperature trends, J. Clim., 18,
94337-4343.
10
11Karoly, D. J., K. Braganza, P. A. Stott, J. M. Arblaster, G. A. Meehl, A. J. Broccoli, and D. W.
12Dixon, 2003: Detection of a human influence on North American climate. Science, 302, 1200–
131203.
14
15Knowles, N., M.D. Dettinger, and D.R. Cayan, 2006: Trends in snowfall versus rainfall for the
16Wester United States, Journal of Climate, 19(8), 4545-4559.
17
18Knutson, T. R., T.L. Delworth, K.W. Dixon, and R.J. Stouffer, 1999: Model assessment of
19regional surface temperature trends (1949-1997). Journal of Geophysical Research. 104(D24),
2030,981-30.996.
21
22Lettenmaier, D. P., and T. Y. Gan, 1990: Hydrologic sensitivities of the Sacramento–San Joaquin
23River Basin, California, to global warming. Water Resour. Res., 26, 69–86.
24
25Liang, X., D. P. Lettenmaier, E. F. Wood, and S. J. Burges, 1994: A Simple hydrologically
26Based Model of Land Surface Water and Energy Fluxes for GSMs, J. Geophys. Res., 99(D7),
2714,415-14,428.
28
29Livezey, R. E., and W. Y. Chen, 1983: Statistical field significance and its determination by
30Monte Carlo techniques. Mon. Wea. Rev., 111, 46–59.
31
32Mantua, N.J., S.R. Hare, Y. Zhang, J.M. Wallace, and R.C. Francis, 1997: A Pacific decadal
33climate oscillation with impacts on salmon. Bulletin of the American Meteorological Society,
34Vol. 78, pp 1069-1079.
35
36Maurer, E. P., A. W. Wood, J. C. Adam, D. P. Lettenmaier, and B. Nijssen, 2002: A long-term
37hydrologically-based data set of land surface fluxes and states for the conterminous United
38States. J. Clim., 15, 3237–3251.
39
40Maurer, E.P., I.T. Stewart, C. Bonfils, P.B. Duffy, D.R. Cayan, 2007: Detection, attribution, and
41sensitivity of trends toward earlier streamflow in the Sierra Nevada. Journal of Geophysical
42Research-Atmospheres, 112, D11118.
43
44Maurer, E. P., and H. G. Hidalgo, 2008: Utility of daily vs. monthly large-scale climate data: an
45intercomparison of two statistical downscaling methods, Hydrol. Earth Syst. Sci.
46
47Meehl, G. A., Hu., A., and B. D. Santer: 2008: The mid 1970s climate shift in the Pacific and the
48relative roles of forced versus inherent decadal variability. Journal of Climate (submitted).

1Mote, P. W., 2003: Trends in snow water equivalent in the Pacific Northwest and their climatic
2causes. *Geophys. Res. Lett.*, 30, 1601, doi:10.1029/2003GL017258.
3
4Mote, P., A. F. Hamlet, M. P. Clark, and D. P. Lettenmaier, 2005: Declining mountain snowpack
5in western North America, *Bull. Am. Meteorol. Soc.*, 86, 39-49.
6
7Mote, P. W., 2006: Climate-driven variability and trends in mountain snowpack in western North
8America. *J. Clim.*, 19, 6209-6220.
9
10Mote, P., Hamlet, A.F., and Salath', E., 2008, Has spring snowpack declined in the Washington
11Cascades? *Hydrol. Earth Syst. Sci.*, 12, 193–206.
12
13Nijssen, B., G. M. O'Donnell, D. P. Lettenmaier, D. Lohmann, and E. F. Wood, 2001: Predicting
14the discharge of global rivers, *J. Clim.*, 14, 3307–3323.
15
16Pierce D.W., T.P. Barnett, H.G. Hidalgo. T. Das, C. Bonfils, B. Sander, G. Bala, M. Dettinger,
17D. Cayan and A. Mirin. 2008: Attribution of declining western US snowpack to human effects. *J.*
18*Climate*, in press.
19
20Regonda, S. K., B. Rajagopalan, M. Clark, and J. Pitlick, 2005: Seasonal cycle shifts in
21hydroclimatology over the western United States. *J. Climate*, 18, 372–384.
22
23Santer, B. D., C. Mears, F. J. Wentz, K. E. Taylor, P. J. Gleckler, T. M. L. Wigley, T. P. Barnett,
24J. S. Boyle, W. Brüggemann, N. P. Gillett, S. A. Klein, G. A. Meehl, T. Nozawa, D. W. Pierce,
25P. A. Stott, W. M. Washington, and M. F. Wehner, 2007: Identification of human-induced
26changes in atmospheric moisture content, *Proc. Nat. Acad. Sc.*, 104, 15248-15253.
27
28Sheffield, J., G. Goteti, F. Wen, and E.F. Wood, 2004: A simulated soil moisture based drought
29analysis for the United States. *Journal of Geophysical Research–Atmospheres*, 109, (D24),
30D24108.
31
32Sheffield, J., and E. F. Wood, 2007: Characteristics of global and regional drought, 1950-2000:
33Analysis of soil moisture data from off-line simulation of the terrestrial hydrologic cycle, *J.*
34*Geophys. Res.*, 112, D17115, doi:10.1029/2006JD008288.
35
36Stewart, I.T., D.R. Cayan and M.D. Dettinger, 2004: Changes in snowmelt runoff timing in
37western North America under a 'Business as Usual' climate change scenario. *Climatic Change*,
3862, 217-232.
39
40Stewart, I.T., D.R. Cayan and M.D. Dettinger, 2005: Changes toward Earlier Streamflow Timing
41across Western North America. *Journal of Climate*, 18, 1136-1155.
42
43The International Ad Hoc Detection and Attribution Group, 2005: Detecting and Attributing
44External Influences on the Climate System: A Review of Recent Advances. *J. Climate*, 18,
451291–1314.
46

1Wood, E.F., D.P. Lettenmaier and V.G. Zartarian, 1992: A land-surface hydrology
2parameterization with subgrid variability for general circulation models, Journal of Geophysical
3Research, pp. 2717–2728.

4

5Wood, A. W., L. R. Leung, V. Sridhar, and D. P. Lettenmaier, 2004: Hydrologic implications of
6dynamical and statistical approaches to downscaling climate model outputs. Climatic Change,
762(1-3), 189-216.

8

9Zhang, X.B., F.W. Zwiers, G.C. Hegerl, F.H. Lambert, N.P. Gillett, S. Solomon, P.A. Stott, T.
10Nozawa, 2007: Detection of human influence on twentieth-century precipitation trends. Nature,
11448 (7152): 461-U4.

12

13Zwiers, F. W., and X. Zhang, 2003: Toward regional-scale climate change detection. J. Climate,
1416, 793–797.

15

16

17

18

19

20

21

22

23

24

25

26

27

28

29

30

31

32

33

34

35

36

37

38

39

40

41

42

43

44

45

46

47

48

1Tables

2

3Table 1

4Areas with significant changes (at 95% confidence level) as a percentage of total area in three

5major tributaries areas of the western U.S. (as shown in Fig. 1b) for four climate variables

6

	California Sierra Nevada	Colorado at the Lees Ferry	Columbia at The Dalles
JFM average temperature	63.3	85.3	88.7
Snowy days as a fraction of wet days	22.3	48.1	35.6
SWE/P _{ONDJFM}	15.2	8.5	24.8
JFM runoff total as a fraction of water year runoff total	5.5	2.9	25.6

7

8

9

10

11

12

13

14

15

16

17

18

19

20

21

1 Figures

2

3 **Fig. 1** (a) Simulation domain showing four major basins/region in the western U.S.; CA:
4 California region (mostly the Sacramento and San Joaquin River basins), GB: Great Basin, CO:
5 Colorado River basin, CL: Columbia River basin; dots represent the outlet of selected
6 catchments. (b) Selected tributaries areas in the western U.S.; SN: Sacramento at Bend Bridge
7 and San Joaquin tributaries, LF: Colorado at the Lees Ferry, DL: Columbia at The Dalles. (c)
8 elevation (in meters above sea level).

9

10 **Fig. 2** Standard deviations of 5-year low pass filtered climate indices obtained using downscaled
11 CCSM3-FV run and gridded observation (for VIC grid cells with at least 50 mm mean value of
12 SWE on 1st April). The observations were linearly detrended before the calculation of standard
13 deviation to remove the part of the possible anthropogenic influence. (a) JFM total precipitation
14 as a fraction of water year total precipitation, (b) JFM average temperature, (c) Snowy days as a
15 fraction of wet days, (d) SWE/P_{ONDJFM} and (e) JFM total runoff as a fraction of water year total
16 runoff

17

18 **Fig. 3** Schematic showing method used to calculate the probability of the JFM average
19 temperature trend being exceeded in the control run. Bars show the distribution of the trends
20 from the control run and the arrow indicates the observed trend. Note if the trend from
21 observation fall within the shaded region indicate the observed trend can be found from the
22 control run simulation at only 5% of the times

23

24 **Fig. 4** (a) Observed trends in monthly average temperature and (b) probabilities of observed
25 trends in monthly average temperature being exceeded in control run trend distribution

26

27 **Fig. 5** Observational trends for the period 1950-1999. (a) JFM average temperature, (b) Snowy
28 days as a fraction of wet days, (c) SWE/P_{ONDJFM} and (d) JFM accumulated runoff as a fraction of
29 water year accumulated runoff.

30

31 **Fig. 6** Same as Fig. 5, except for the probabilities of the observational trends (as shown in Fig. 5)
32 being exceeded by trends from the model control run. Percentage in upper right are fractions of
33 VIC grid cells significantly different from the control run at 95% confidence level, and, in
34 parenthesis, the percentage that could occur due to randomness (obtained from the Monte Carlo
35 resampling) (a) JFM average temperature, (b) Snowy days as a fraction of wet days, (c)
36 SWE/P_{ONDJFM} and (d) JFM total runoff as a fraction of water year total runoff

37

38 **Fig. 7** Accumulated number of grid cells as a fraction of total grid cells in each elevation class.
39 On left, red points show the results with positive trends. On right, blue colours show the results
40 with negative trends. Light black regions indicate that results not significant from the control run
41 at the 95% level (using the Monte Carlo resampling method). (a) JFM total precipitation as a
42 fraction of water year total precipitation, (b) JFM average temperature, (c) Snowy days as a
43 fraction of wet days, (d) SWE/P_{ONDJFM} and (e) JFM total runoff as a fraction of water year total
44 runoff

45

46 **Fig. 8** Same as Fig. 7, except the grid cells are categorized according to MAM temperature class.
47 (a) JFM total precipitation as a fraction of water year total precipitation, (b) JFM average

1 temperature, (c) Snowy days as a fraction of wet days, (d) SWE/P_{ONDJFM} and (e) JFM total runoff
2 as a fraction of water year total runoff

3

4 **Fig. 9** Same as Fig. 7, except the grid cells are accumulated over different time intervals. Left
5 panel shows results when analysis period was 30 years, 40 years and 50 years, all beginning
6 1950. Right panel shows results for three different 30 year periods having different starting years,
7 1950, 1960 and 1970. As before the magnitude of the observed trends are compared to those
8 from an ensemble of segments of the control run having the same record length. Red points show
9 the results with significant (at 95% confidence level) positive trends, blue colours show the
10 results with significant negative trends, and light black colours symbols show results that were
11 not significant from the control run using the Monte Carlo resampling method. (a) JFM average
12 temperature, (b) SWE/P_{ONDJFM} and (c) JFM total runoff as a fraction of water year total runoff
13

14 **Fig. 10** Ordinate shows, for aggregate over a catchment, the probability of that observed trends
15 are different from those from control run, plotted against (abscissa), the percentage of grid
16 points within a catchment having observed trends significantly (at 95% confidence level) greater
17 than those from control run trends. (a) JFM average temperature, (b) Snowy days as a fraction of
18 wet days, (c) SWE/P_{ONDJFM} and (d) JFM total runoff as a fraction of water year total runoff. In
19 the figures “squares”, “×” and “circles” symbols show the results for the catchments located in
20 the Columbia River basin, Colorado River basin and California region (as shown in Fig. 1a),
21 respectively. Symbols within shaded region indicate the observed trends (at the catchment scale)
22 different than the model control run trends distribution at 95% confidence level.

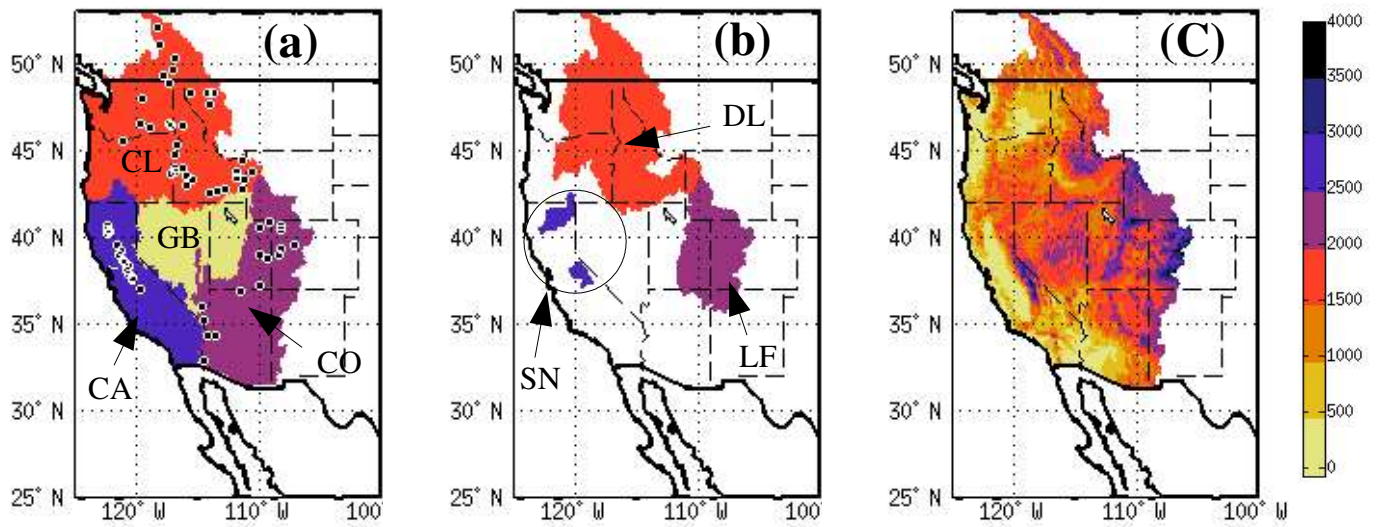


Fig. 1 (a) Simulation domain showing four major basins/region in the western U.S.; CA: California region (mostly the Sacramento and San Joaquin River basins), GB: Great Basin, CO: Colorado River basin, CL: Columbia River basin; dots represent the outlet of selected catchments. (b) Selected tributaries areas in the western U.S.; SN: Sacramento at Bend Bridge and San Joaquin tributaries, LF: Colorado at the Lees Ferry, DL: Columbia at The Dalles. (c) elevation (in meters above sea level)

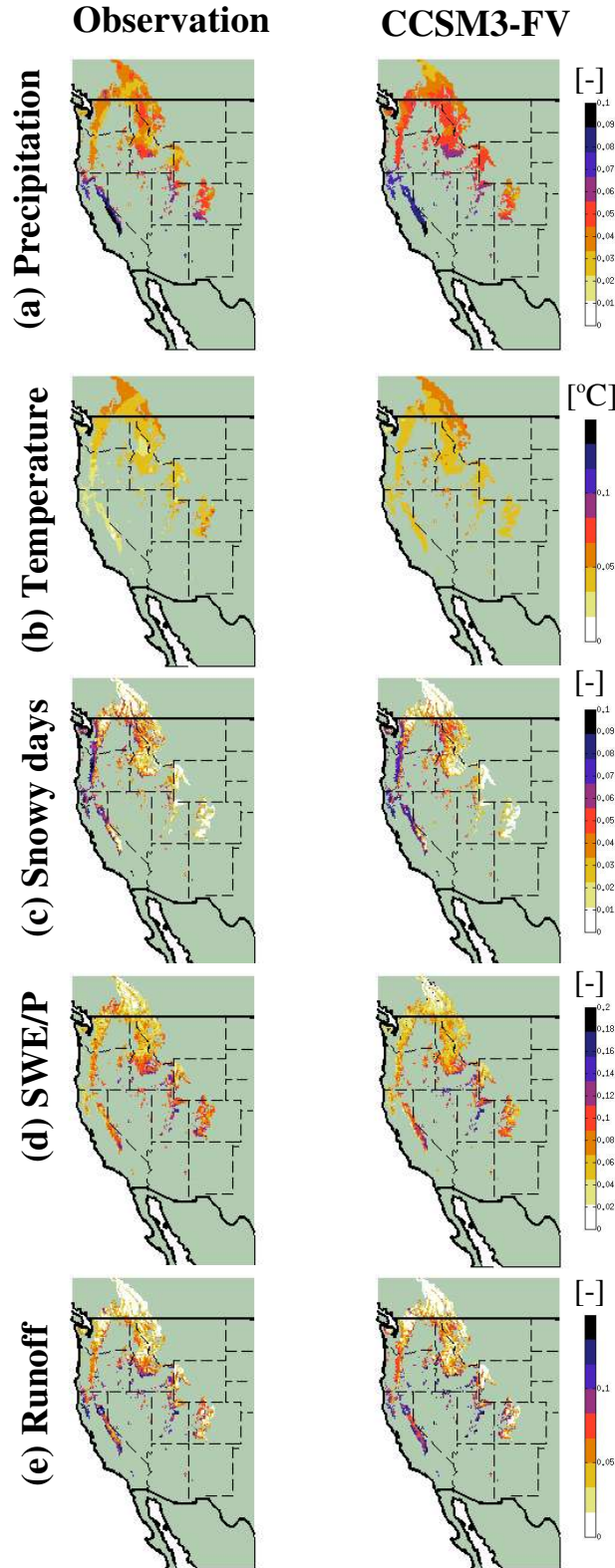


Fig. 2 Standard deviations of 5-years low pass filtered climate indices obtained using downscaled CCSM3-FV run and gridded observation (for VIC grid cells with at least 50 mm mean value of SWE on 1st April). The observations were linearly detrended before the calculation of standard deviation to remove the part of the possible anthropogenic influence. (a) JFM total precipitation as a fraction of water year total precipitation, (b) JFM average temperature, (c) Snowy days as a fraction of wet days, (d) SWE/P_{ONDJFM} and (e) JFM total runoff as a fraction of water year total runoff

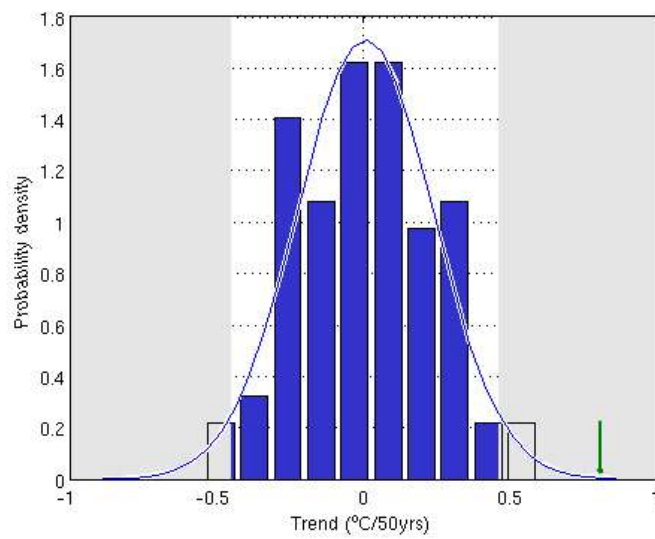


Fig. 3 Schematic showing method used to calculate the probability of the JFM average temperature trend being exceeded in the control run. Bars show the distribution of the trends from the control run and the arrow indicates the observed trend. Note if the trend from observation fall within the shaded region indicate the observed trend can be found from the control run simulation at only 5% of the times

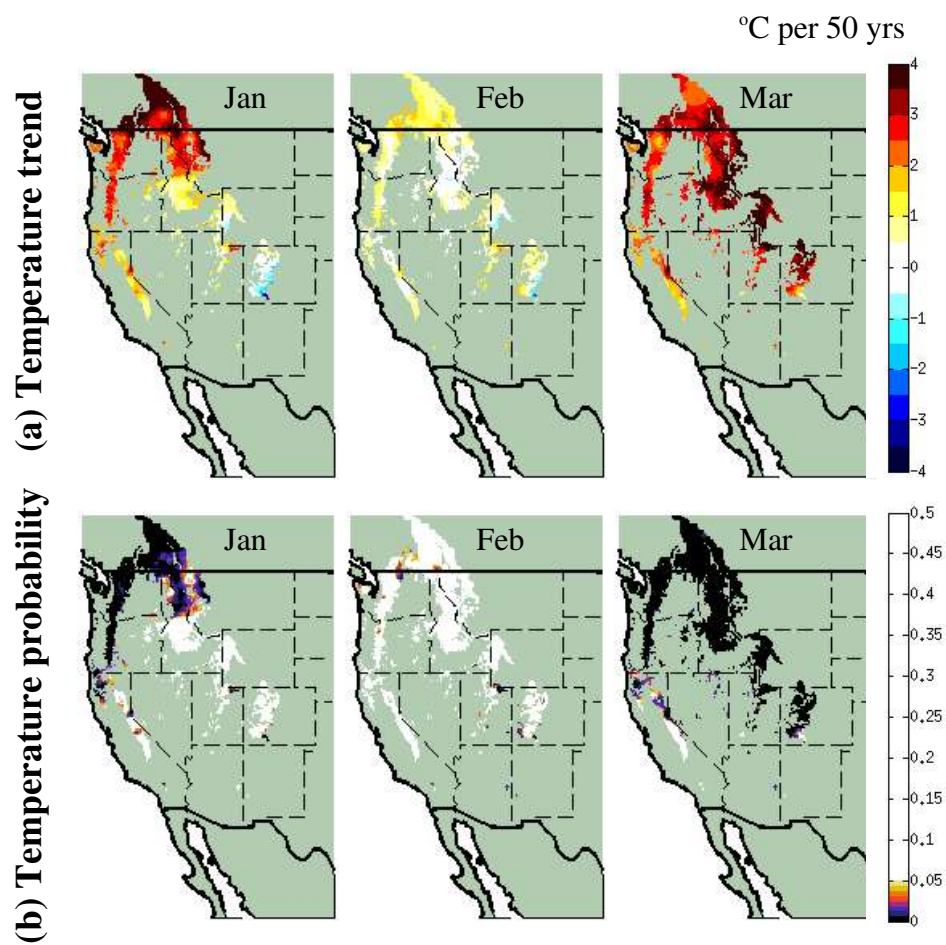


Fig. 4 (a) Observed trends in monthly average temperature and (b) probabilities of observed trends in monthly average temperature being exceeded in control run trend distribution

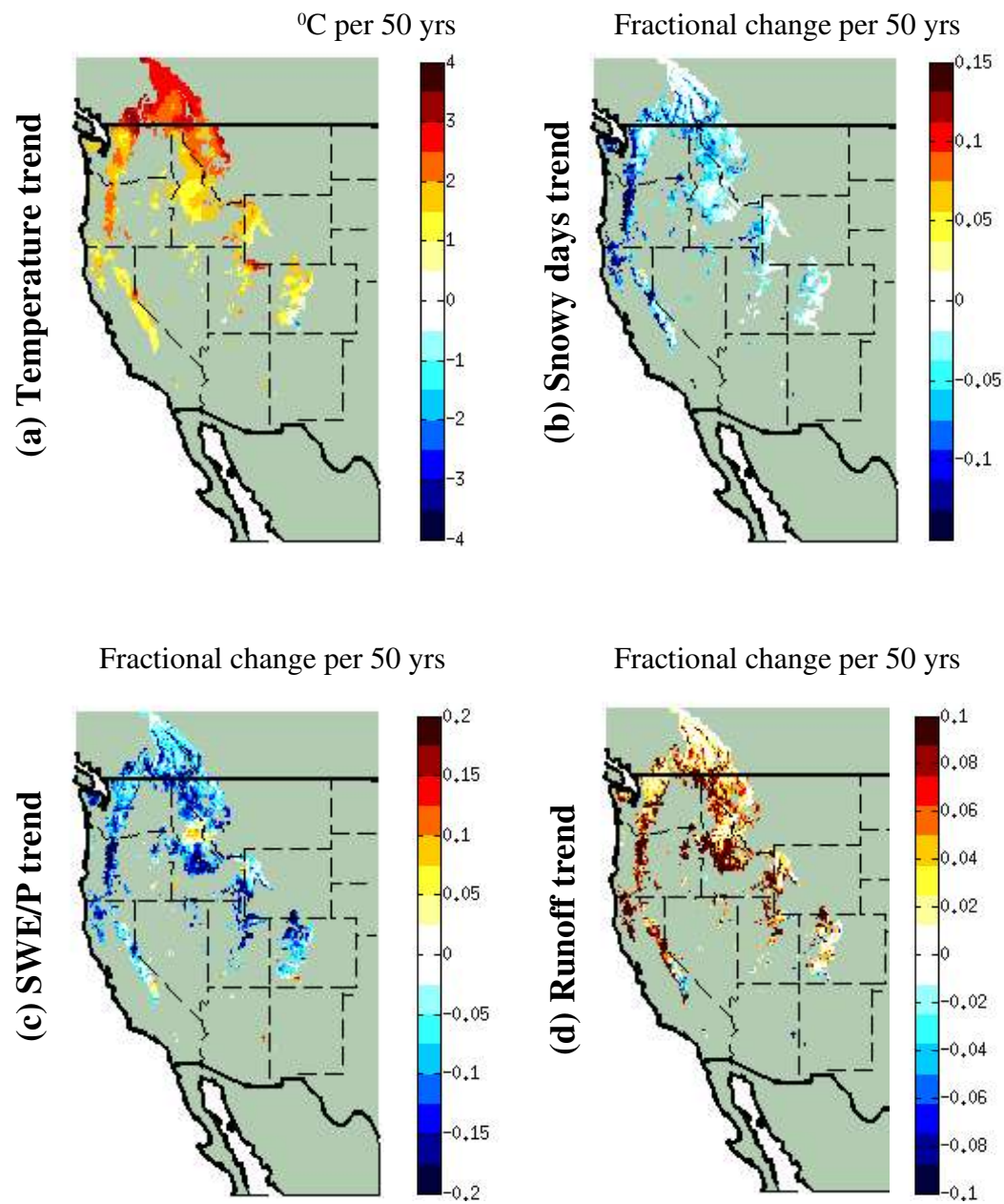


Fig. 5 Observational trends for the period 1950-1999. (a) JFM average temperature, (b) Snowy days as a fraction of wet days, (c) $\text{SWE}/P_{\text{ONDJFM}}$ and (d) JFM accumulated runoff as a fraction of water year accumulated runoff

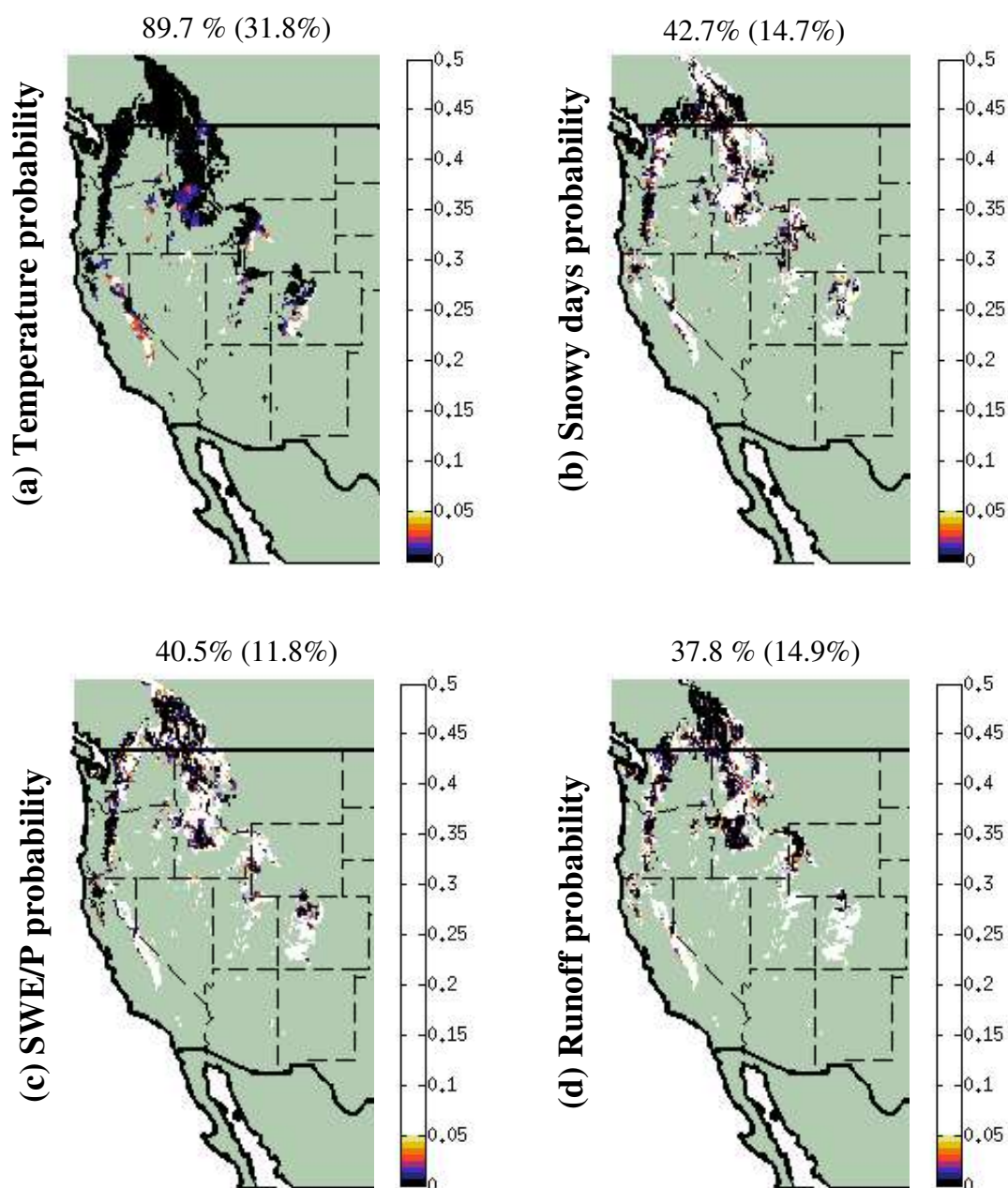
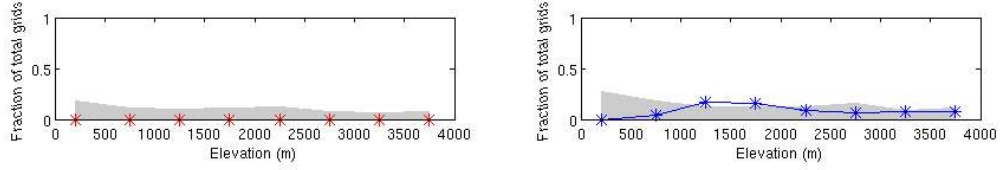
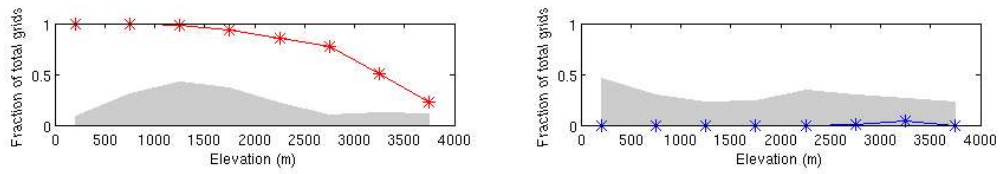


Fig. 6 Same as Fig. 5, except for the probabilities of the observational trends (as shown in Fig. 5) being exceeded by trends from the model control run. Percentage in upper right are fractions of VIC grid cells significantly different from the control run at 95% confidence level, and, in parenthesis, the percentage that could occur due to randomness (obtained from the Monte Carlo resampling) (a) JFM average temperature, (b) Snowy days as a fraction of wet days, (c) SWE/ P_{ONDJFM} and (d) JFM accumulated runoff as a fraction of water year accumulated runoff

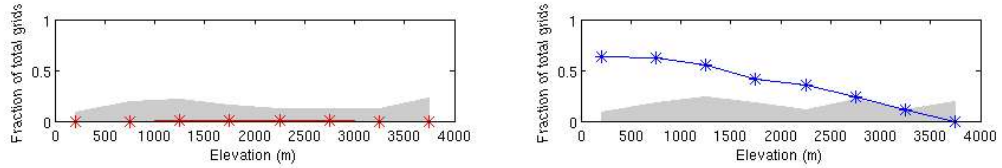
(a) Precipitation



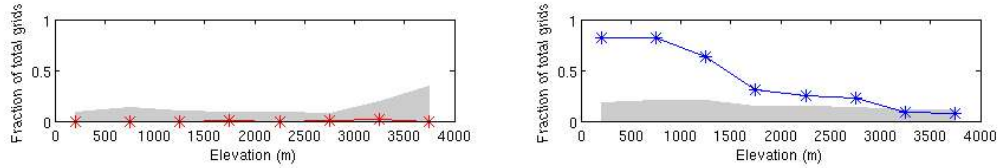
(b) Temperature



(c) Snowy days



(d) SWE/P



(e) Runoff

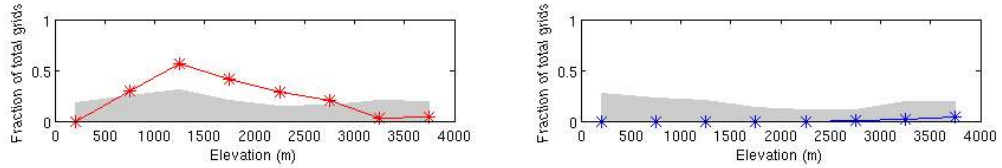


Fig. 7 Accumulated number of grid cells as a fraction of total grid cells in each elevation class. On left, red points show the results with positive trends. On right, blue colours show the results with negative trends. Shaded regions indicate that results not significant from the control run at the 95% level (using the Monte-Carlo resampling method). (a) JFM total precipitation as a fraction of water year total precipitation, (b) JFM average temperature, (c) Snowy days as a fraction of wet days, (d) $\text{SWE/P}_{\text{ONDJFM}}$ and (e) JFM accumulated runoff as a fraction of water year accumulated runoff

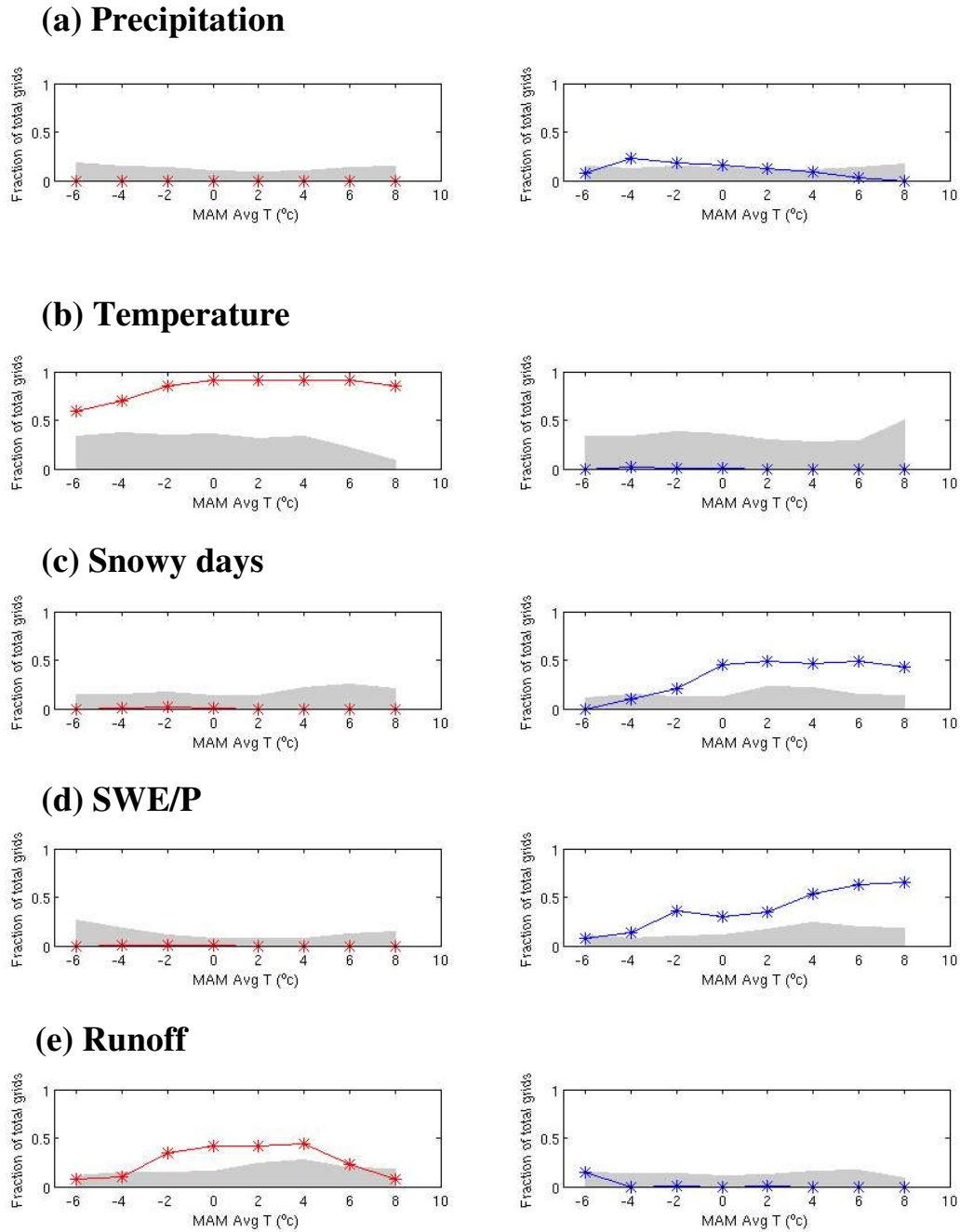


Fig. 8 Same as Fig. 7, except the grid cells are categorized according to MAM (March-April-May) temperature class. a) JFM total precipitation as a fraction of water year total precipitation, (b) JFM average temperature, (c) Snowy days as a fraction of wet days, (d) SWE/P_{ONDJFM} and (e) JFM accumulated runoff as a fraction of water year accumulated runoff

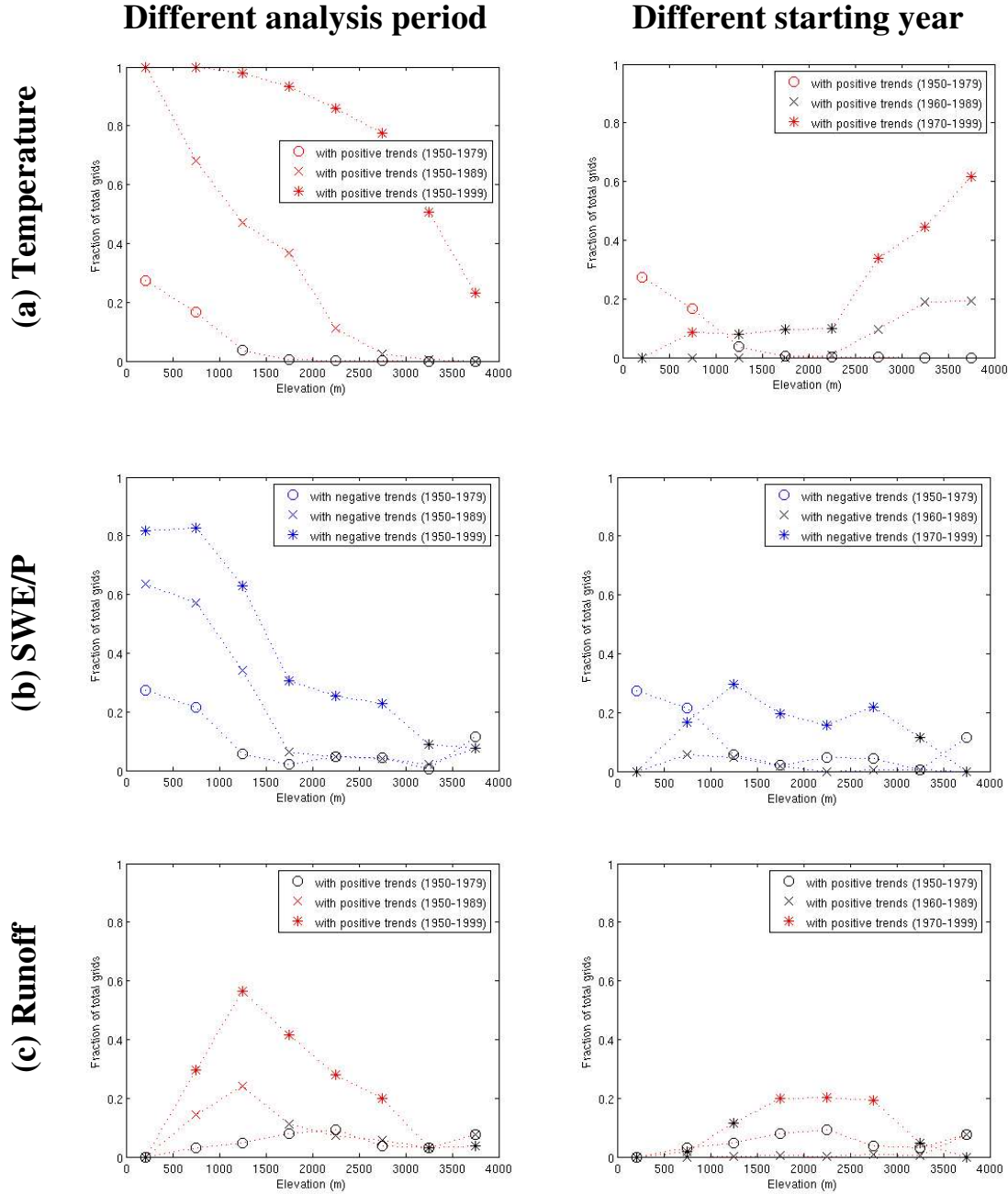
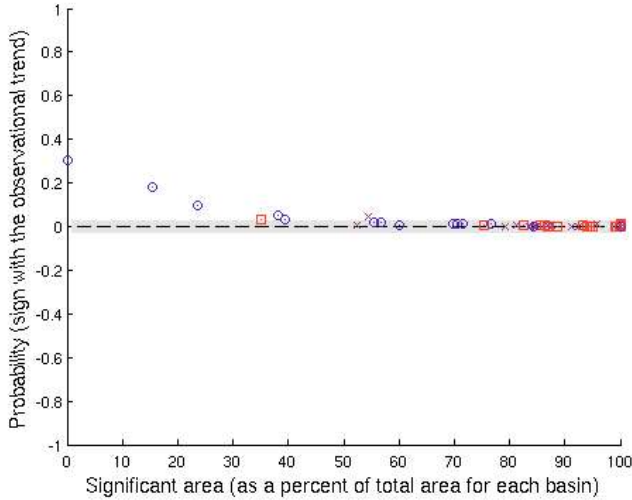
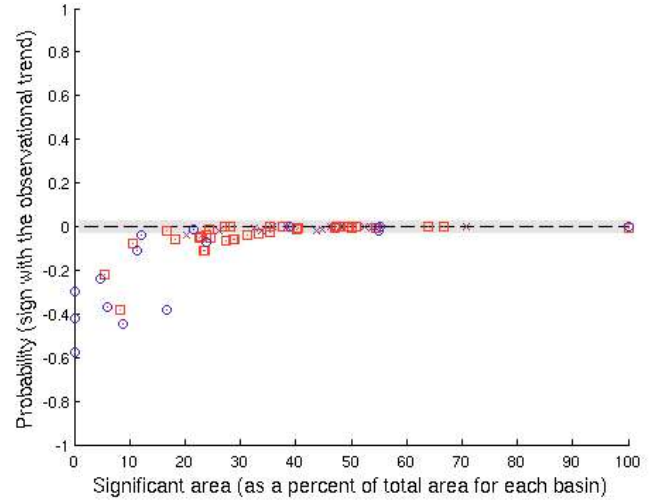


Fig. 9 Same as Fig. 7, except the grid cells are accumulated over different time intervals. Left panel shows results when analysis period was 30 years, 40 years and 50 years periods, all beginning 1950. Right panel shows results for three different 30 year periods having different starting years, 1950, 1960 and 1970. As before the magnitude of the observed trends are compared to those from an ensemble of segments of the control run having the same record length. Red points show the results with significant (at 95% confidence level) positive trends, blue colours show the results with significant negative trends, and black colours symbols show results that were not significant from the control run using the Monte Carlo resampling method. (a) JFM average temperature, (b) SWE/P_{ONDJFM} and (c) JFM accumulated runoff as a fraction of water year accumulated runoff

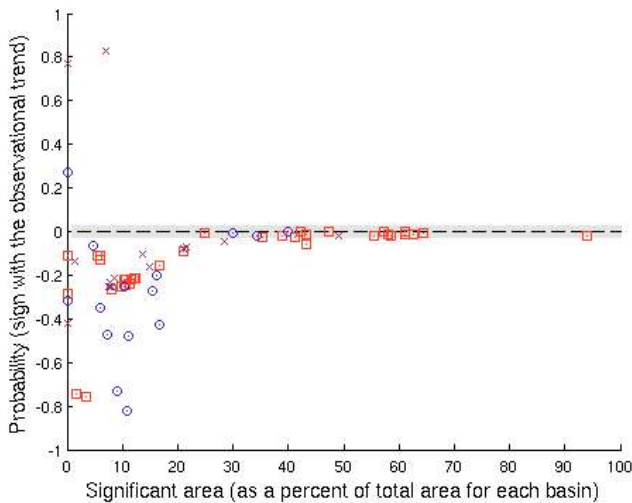
(a) Temperature



(b) Snowy days



(c) SWE/P



(d) Runoff

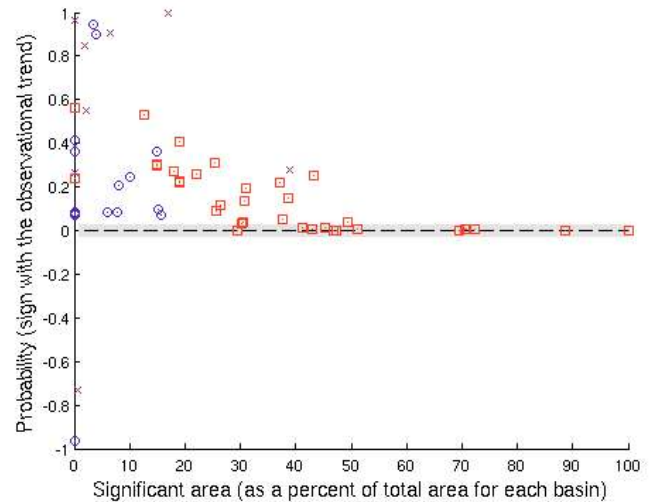


Fig. 10 Ordinate shows, for aggregate over a catchment, the probability of that observed trends are different from those from control run, plotted against (abscissa), the percentage of grid cells within a catchment having observed trends significantly (at 95% confidence level) greater than those from control run trends. In the figures the probability was multiplied by the sign of the observed trend to indicate the observed trend direction. (a) JFM average temperature, (b) Snowy days as a fraction of wet days, (c) $\text{SWE/P}_{\text{ONDJFM}}$ and (d) JFM total runoff as a fraction of water year total runoff. In the figures “squares”, “x” and “circles” symbols show the results for the catchments located in the Columbia River basin, Colorado River basin and California region (as shown in Fig. 1a), respectively. Symbols within shaded region indicate the observed trends (at the basin scale) are different from the model control run trend at 95% confidence level.